J Vet Intern Med 2010;24:918–931

Quantitative Analysis of Stress Echocardiograms in Healthy Horses with 2-Dimensional (2D) Echocardiography, Anatomical M-Mode, Tissue Doppler Imaging, and 2D Speckle Tracking

K.D. Schefer, C. Bitschnau, M.A. Weishaupt, and C.C. Schwarzwald

Background: Stress echocardiography is used to diagnose myocardial dysfunction in horses, but current methods are not well standardized. The influence of heart rate (HR) on measurements is largely unknown.

Objectives: To investigate the use of 2-dimensional echocardiography (2DE), anatomical M-mode (AMM), tissue Doppler imaging (TDI), and 2D speckle tracking (2DST) at rest and after exercise for quantification of regional and global left-ventricular (LV) function.

Animals: Five athletic Warmblood horses; 11.6 ± 3.6 years; 529 ± 48 kg.

Methods: Prospective study. Three separate echocardiographic examinations were performed before (baseline) and over 5 minutes after treadmill exercise with 2DE (1st, short-axis view; 2nd, long-axis view) and pulsed-wave TDI (3rd examination). Offline analyses were performed at baseline and after exercise at HR 120, 110, 100, 90, and 80 $minute^{-1}$. Global and segmental measurements were compared by analysis of variance.

Results: Quantitative analyses of stress echocardiograms were feasible in all horses. None of the AMM indices changed significantly after exercise. Stroke volume and ejection fraction by 2DE and strain by 2DST decreased, whereas strain rate by 2DST increased significantly at HR > 100 $minute^{-1}$. TDI analyses were technically difficult and provided little additional information.

Conclusions and Clinical Importance: Volumetric indices by 2DE and strain and strain rate by 2DST are applicable for quantitative assessment of stress echocardiograms. In healthy horses, they are significantly altered at a HR > 100 $minute^{-1}$ and need to be evaluated in view of the instantaneous HR. Further investigations are needed to define the clinical value of stress echocardiography in horses with cardiac disease.

Key words: Cardiology; Performance evaluation; Treadmill stress testing.

Heart disease is recognized as a potential cause of exercise intolerance and poor performance in athletic horses.[1] The diagnosis of performance-limiting heart disease is complicated by the high prevalence of heart murmurs and of valvular regurgitation detected by color Doppler echocardiography in apparently healthy horses.[2,3] Furthermore, myocardial disease can exist in the absence of murmurs or dysrhythmias and might therefore be underrecognized.[4,5] Despite recent advances in cardiovascular diagnostics, it is often difficult to prove an etiologic relationship between echocardiographic findings and impaired athletic performance unless severe valvular regurgitation, significant chamber enlargement, obvious myocardial dysfunction, or marked cardiac dysrhythmia can be diagnosed.

Stress echocardiography has gained interest in equine medicine, with the goal to diagnose stress-induced myocardial dysfunction.[4,6–12] However, the incidence of exercise-induced myocardial ischemia is largely unknown in horses, the target diseases to be detected are not well defined, and the indications for stress echocardiography and its clinical value in horses are still unresolved. Fur-

From the Equine Department, Vetsuisse Faculty (Schefer, Bitschnau, Weishaupt, Schwarzwald), and the Zurich Center for Integrative Human Physiology (ZIHP) (Schwarzwald), University of Zurich, Zurich, Switzerland.

Corresponding author: Colin C. Schwarzwald, PD Dr med vet, PhD, Dipl ACVIM, Equine Department, Vetsuisse Faculty, University of Zurich, Winterthurerstrasse 260, 8057 Zurich, Switzerland; e-mail: cschwarzwald@vetclinics.uzh.ch.

Submitted October 21, 2009; Revised January 25, 2010; Accepted April 15, 2010.

10.1111/j.1939-1676.2010.0542.x

Abbreviations:

2D	2-dimensional
2DE	2-dimensional echocardiography
2DST	2-dimensional speckle tracking
A_m	late-diastolic radial wall motion velocity
AMM	anatomical M-mode
CO	cardiac output
cTDI	color tissue Doppler imaging
D_{L-sys}	longitudinal peak systolic displacement
D_{R-sys}	radial peak systolic displacement
E_1	isovolumic relaxation velocity
EF	ejection fraction
E_m	early-diastolic radial wall motion velocity
EMS	electromechanical systole
ET	ejection time
ε_L	longitudinal peak strain
ε_R	radial peak strain
FAC	fractional area change
FC	fractional change
FS	fractional shortening
HR	heart rate
IMP	index of myocardial performance (Tei index)
IVCT	isovolumic contraction time
IVRT	isovolumic relaxation time
IVS	interventricular septum
IVSd	interventricular septal thickness at end-diastole
IVSs	interventricular septal thickness at peak systole
LAX	long axis
LV	left ventricle or left-ventricular
LVEAd	left-ventricular external area at end-diastole
LVEAs	left-ventricular external area at peak systole
LVFW	left-ventricular free wall
LVFWd	left-ventricular free wall at end-diastole
LVFWs	left-ventricular free wall at peak systole
LVIAd	left-ventricular internal area at end-diastole

LVIAs	left-ventricular internal area at peak systole
LVIDd	left-ventricular internal diameter at end-diastole
LVIDs	left-ventricular internal diameter at peak systole
LVIVd	left-ventricular internal volume at end-diastole
LVIVs	left-ventricular internal volume at peak systole
LVMA FC	fractional change in left-ventricular myocardial area
LVMAd	left-ventricular myocardial area at end-diastole
LVMAs	left-ventricular myocardial area at peak systole
MRI	magnetic resonance imaging
MV	mitral valve
MWT_A FC	fractional change in mean wall thickness
MWT_Ad	mean wall thickness at end-diastole (calculated from 2D SAX area measurements)
MWT_As	mean wall thickness at peak systole (calculated from 2D SAX area measurements)
MWTd	mean wall thickness at end-diastole (calculated from AMM measurements)
MWTs	mean wall thickness at peak systole (calculated from AMM measurements)
PEP	pre-ejection period
PW TDI	pulsed-wave tissue Doppler imaging
ROI	region of interest
RWT_Ad	relative wall thickness at end-diastole (calculated from 2D SAX area measurements)
RWTd	relative wall thickness at end-diastole (calculated from AMM measurements)
S_I	isovolumic contraction velocity
SAX	short axis
S_m	systolic radial wall motion velocity during ejection
SR_{L-sys}	longitudinal peak systolic strain rate
SR_{R-sys}	radial peak systolic strain rate
$STI\varepsilon_R$	synchrony time index
SV	stroke volume
SVA	subjective visual assessment
$tAVC_a$	time of aortic valve closure (automatically determined)
TDI	tissue Doppler imaging
$t\varepsilon_L$	time to longitudinal peak strain
$t\varepsilon_R$	time to radial peak strain

thermore, there is a paucity of standardized and objective methods for assessment of left-ventricular (LV) function after stress induction in horses.

Quantitative assessment of *global* LV function after exercise is currently limited to measurement of chamber dimensions and calculation of ejection phase indices derived from 2-dimensional (2D) or M-mode images. However, the current literature is inconsistent in regards to the time course of commonly used measurements after treadmill exercise,[4,6,9,11] suggesting that many of them might not be suitable for quantitative assessment of stress echocardiographic studies. Assessment of *regional* myocardial function is even more difficult. It has been achieved by manual tracking of endocardial motion and subjective evaluation of regional wall motion.[4,12,13] However, truly quantitative approaches have not been established in horses.

Finally, the influence of heart rate (HR) on echocardiographic indices of cardiac function has not been thoroughly investigated to date,[4,6,9,11] although it is generally recommended to perform stress echocardiography in horses immediately after cessation of treadmill exercise, at an HR above 100 minute^{-1}.[4]

Advanced echocardiographic techniques might serve to overcome some of the current limitations of equine stress echocardiography. Anatomical M-mode (AMM)[a] allows offline analysis of conventional 2D cineloop recordings, reducing the time required for data collection.[14,15]Area-based measurements allow assessment of shortening in two dimensions and are less sensitive to asynchronous wall motion,[16,17] while volume-based indices are generally considered most accurate and least affected by altered chamber geometry.[16–19] Tissue Doppler imaging (TDI) has recently been used to study left atrial and LV wall motion in resting horses[20–23] and might serve to quantify LV systolic and diastolic function and to detect occult myocardial disease.[24–29] Finally, 2D speckle tracking (2DST) allows quantitative assessment of regional and global systolic LV wall motion in longitudinal and radial direction based on conventional 2DE cineloop recordings.[24,30–32]

The goal of this study was to investigate the changes over time of echocardiographic indices of LV systolic function within the 1st 5 minutes after cessation of a standardized treadmill exercise test in athletic horses using 2DE, AMM, TDI, and 2DST. The influence of HR on indices of LV function was investigated, to determine the potential clinical value of each index and to identify a HR limit above which stress echocardiography should be performed. We hypothesized that the indices of LV function largely depend on HR and are highly variable within the first 5 minutes after treadmill exercise.

Material and Methods

Study Population

Five adult 3-day event horses (all Warmbloods; 2 mares, 3 geldings) in athletic condition, aged 11.6 ± 3.6 years (mean ± SD) and with a body weight of 529 ± 48 kg, were studied prospectively. All horses were considered healthy based upon physical examination, CBC, plasma fibrinogen concentration, serum biochemistry profile, and routine transthoracic echocardiography. None of the horses received medications during the 2 weeks preceding entry into the study. The horses were accustomed to the treadmill over a 2-day period with at least 4 training sessions lasting 30–40 minutes each. The study was approved by the district veterinary office of the canton Zurich.

Study Design

Each horse underwent 3 standardized multistep exercise tests on a high-speed treadmill[b] within 69 ± 29 days. Stress echocardiographic recordings were obtained on each of the 3 occasions.

Exercise Test

The horses underwent a submaximal incremental exercise test on a 6% inclined treadmill. Before starting the exercise test, the horses were warmed up for approximately 30 minutes at all 3 gaits. The exercise test consisted of 1–2 steps at trot (3.5 or 4.0 m/s) and 4–5 steps at canter and gallop (6.0–10.0 m/s) depending on the performance capacity of the horse. Speed increments were 1 m/s. The 1st step lasted 2 minutes and the subsequent steps 90 seconds. The horses were not run to fatigue. The exercise test was terminated

when horses reached a speed at which the blood lactate concentration was >4 mmol/L. The time from peak exercise to complete stop of the treadmill was 30 seconds. The treadmill was then stopped for 5 minutes of passive recovery and recording of the echocardiographic images. Thereafter, the horses walked for active cool-down.

Echocardiography

Transthoracic echocardiography was performed with a high-end digital echocardiograph[c] with a phased-array transducer[d] at a frequency of 1.7/3.6 MHz (octave harmomics). A single-lead base-apex ECG was recorded simultaneously for timing. All echocardiographic recordings were performed by the same operator (C.C.S.) according to a standard protocol. During each of the 3 occasions, stress-echocardiographic recordings were obtained in a single imaging plane. The 1st examination consisted of 2DE recordings in a right parasternal short-axis (SAX) view at the level of the chordae tendineae. The 2nd examination consisted of 2DE recordings in a right parasternal 4-chamber long-axis (LAX) view. For all 2DE recordings, the imaging depth was 28 cm and the sector width was reduced 1 step from its maximum width, to achieve a frame rate of 53.9 frames/s in 2DE mode. The 3rd examination consisted of pulsed-wave TDI (PW TDI) recordings of the LV free wall (LVFW) in a right parasternal SAX view at the level of the chordae tendineae. A sample width of 5.9 mm was used. The sample was placed on the LVFW, so that it covered the subendocardial region during diastole and stayed on the myocardium during the entire cardiac cycle. The velocity scale was set to −50 to +50 cm/s. The simultaneous 2D image was frozen during the PW TDI recordings. Echocardiographic recordings were conducted immediately before (baseline) and continuously over 5 minutes after the exercise test with the horse standing still on the treadmill, being restrained by an experienced handler. The echocardiographic recordings were stored as cine-loops (2DE) or as still images (PW TDI) in digital raw-data format for subsequent offline analyses.

Data Analysis

Data analysis was performed offline, in random order, and with the observer (K.D.S.) blinded to signalment and previous measurements, using a dedicated software package.[a] Measurements were performed on prestress recordings (baseline) and on poststress recordings at predetermined target HR of 120 minute^{-1} (range 115–124 minute^{-1}; HR_{120}), 110 minute^{-1} (range 105–114 minute^{-1}; HR_{110}), 100 minute^{-1} (range 95–104 minute^{-1}; HR_{100}), 90 minute^{-1} (range 85–94 minute^{-1}; HR_{90}), and 80 minute^{-1} (range 75–84 minute^{-1}; HR_{80}). Three nonconsecutive cardiac cycles were analyzed for each variable and at each target HR, and the average of the 3 measurements was used for further analyses.

Standard LV measurements were performed on the right parasternal SAX recordings by AMM techniques.[b] The following variables were measured: the interventricular septal thickness (IVSd, IVSs), the LV internal diameter (LVIDd, LVIDs), and the LV free wall thickness (LVFWd, LVFWs) by the "trailing-inner inner-leading edge" method. End-diastolic measurements (d) were performed at the peak of the electrocardiographic R wave, because the onset of the R wave was not always clearly discernible. Systolic measurements (s) were taken at peak systole, at the time of maximum excursion of IVS and LVFW, respectively. The relative wall thickness at end-diastole (RWTd) was calculated as RWTd = (IVSd + LVFWd) / LVIDd. The mean wall thickness at end-diastole (MWTd) and at peak systole (MWTs) was calculated as MWTd = (IVSd + LVFWd) / 2 and MWTs = (IVSs + LVFWs) / 2, respectively. The LV fractional shortening (FS) was calculated as an index of LV systolic function by the following equation: FS (%) = (LVIDd − LVIDs) / LVIDd × 100.

LV area measurements were performed on the right parasternal SAX recordings. The internal LV area (LVIAd, LVIAs) and the external LV area (LVEAd, LVEAs) were measured at end-diastole (d) and at peak systole (s) by tracing the internal and the external border of the myocardium. The duration of the electromechanical systole (EMS) was measured as the time interval from the electrocardiographic peak R wave to the time of peak systole, defined as the time of maximum excursion of IVS and LVFW. The LV myocardial area at end-diastole (LVMAd) and at peak systole (LVMAs) was calculated as LVMAd = LVEAd − LVIAd and LVMAs = LVEAs − LVIAs, respectively. The mean wall thickness at end-diastole (MWT_Ad) and at peak systole (MWT_As) was calculated as $MWT_A d = \sqrt{(LVEAd / \pi)} - \sqrt{(LVIAd / \pi)}$ and $MWT_A s = \sqrt{(LVEAs / \pi)} - \sqrt{(LVIAs / \pi)}$, respectively. The relative wall thickness at end-diastole (RWT_Ad) was calculated as $RWT_A d = [\sqrt{(LVEAd / \pi)} - \sqrt{(LVIAd / \pi)}] / \sqrt{(LVIAd / \pi)}$.

Indices of LV systolic function were calculated from the area-based measurements: The LV fractional area change [LV FAC (%) = (LVIAd − LVIAs) / LVIAd × 100], a surrogate of LV ejection fraction (EF); the fractional change (FC) in mean wall thickness [MWT_A FC (%) = ($MWT_A s - MWT_A d$) / $MWT_A d \times 100$] and the FC in LV myocardial area [LVMA FC = (LVMAs − LVMAd) / LVMAd], 2 indices of myocardial deformation (ie, myocardial strain); and the MWT_A FC/EMS ratio and the LVMA FC/EMS ratio, 2 indices reflecting the rate of myocardial deformation (ie, myocardial strain rate).

Left-ventricular internal volume at end-diastole (LVIVd) and LV internal volume at peak systole (LVIVs) were calculated based on LAX recordings by the single-plane Simpson's method.[19] The HR of each measured cycle was calculated based on the RR interval (HR = 60,000 / RR). The stroke volume [SV = LVIVd − LVIVs], the LV EF [EF (%) = (LVIVd − LVIVs) / LVIVd × 100], and the cardiac output [CO = SV × HR] were calculated as indices of LV systolic function.

The 2DST analyses were performed by the 2D strain module of the analysis software[a] as described elsewhere.[32] The measurements were obtained from the same cycles as used for 2DE and AMM analyses. The SAX 2DE recordings were analyzed using the "SAX-MV" option and the LAX 2DE recordings were analyzed using the "4CH" option of the 2D strain module. The region of interest (ROI) was determined by tracing the endocardial border of the LV at end-systole. For SAX recordings, tracing was started at midseptum and proceeded in a clockwise direction. For LAX recordings, tracing started at the septal mitral valve (MV) annulus and ended at the lateral MV annulus. The papillary muscles were not included in the LAX tracings. The ROI width was adjusted so that the entire myocardial thickness was covered throughout the cardiac cycle. Six myocardial segments were automatically determined by the software based on regional wall motion analysis standards applied to human patients and were not adjusted for use in the horse (details regarding the position of the different segments are described elsewhere[32]). The quality of systolic tracking was visually assessed by the operator. Thereby, the cycle was replayed in slow-motion and accurate tracking (in particular tracking of the endocardial border) was assessed. If necessary, the line tracing of the endocardium was adjusted and the speckle tracking analysis was repeated until adequate tracking was confirmed by the software. If adequate tracking was not possible despite repeated adjustments of the ROI, another cardiac cycle was chosen for analysis. If adequate tracking was not possible in any cardiac cycle of the target HR, the inadequately tracked segment was excluded from further analysis. Six curve profiles were obtained in each view, corresponding to the average of each of the 6 myocardial segments. The time from the beginning of the cycle (electrocardiographic R wave) to aortic valve closure ($tAVC_a$) was automatically determined and displayed by the software. The measurements for strain (%), strain rate (1/s), and displacement (mm) were performed on the "Results" screen of the

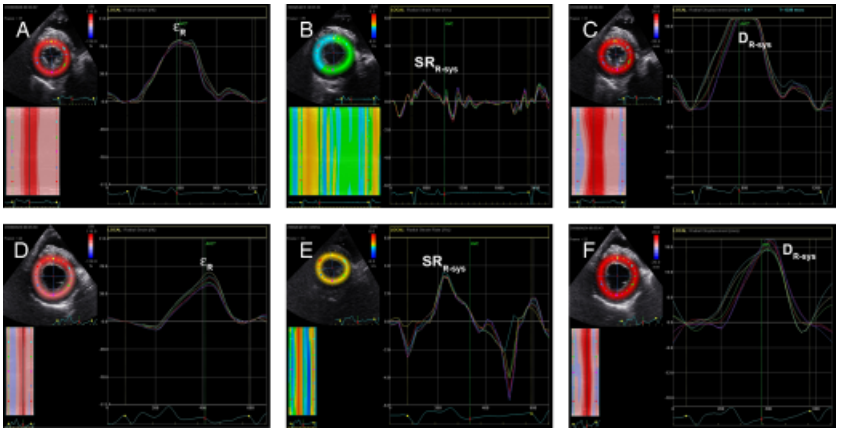

Fig 1. Two-dimensional speckle tracking (2DST) analyses of the left ventricle in short-axis recordings. Trace screens of the 2DST software are shown, displaying the following information: Top left, 2D image with the segmented region of interest (ROI) and parametric color coding at the time of aortic valve closure. Bottom left, M-mode with parametric color coding. Right, Trace display for the selected index. The horizontal axis represents the time in ms, the vertical axis represents the selected index. Notice that the scale of the vertical axis is the same in the trace displays of baseline recordings (**A**–**C**) as in the trace displays of the corresponding postexercise recordings (**D**–**F**). The colors of the trace correspond to the colors of the segmented ROI. The dotted line (where shown) indicates the instantaneous average of all segments at the respective time of the cardiac cycle. An ECG is superimposed for timing. The start and the end of the cycle (R waves) are marked on the ECG with yellow dots. The $tAVC_a$ is indicated by a green vertical line, dividing the cycle in its systolic and diastolic components. (**A**) Radial strain at baseline. (**B**) Radial strain rate at baseline. (**C**) Radial displacement at baseline. (**D**) Radial strain at HR_{120}. (**E**) Radial strain rate at HR_{120}. (**F**) Radial displacement at HR_{120}. ε_R, radial peak strain; SR_{R-sys}, radial peak systolic strain rate; D_{R-sys}, radial peak systolic displacement.

2D Strain software module, using the default settings for spacial smoothing, temporal smoothing, and drift-compensation. Automated detection of the peak values was verified on the graphical display and manually corrected by the observer as necessary. The indices measured in this study were chosen based upon the results of a previous investigation on the use of 2DST in horses.[32] In SAX recordings, the following indices of LV function were measured: Radial peak strain (peak independent of aortic valve closure; ε_R), time from beginning of the cardiac cycle to ε_R ($t\varepsilon_R$), radial peak systolic strain rate (SR_{R-sys}), and radial peak systolic displacement (D_{R-sys}) (Fig 1A–F). In LAX recordings, the following indices of LV function were measured: Longitudinal peak strain (peak independent of aortic valve closure; ε_L), time from beginning of the cardiac cycle to ε_L ($t\varepsilon_L$), longitudinal peak systolic strain rate (SR_{L-sys}), and longitudinal peak systolic displacement (D_{L-sys}) (Fig 2A–F). The $tAVC_a$ and the electrocardiographic RR interval were measured for each cycle. The corresponding instantaneous HR was calculated as 60,000 / RR interval.

Evaluation of myocardial synchrony was achieved by subjective visual assessment (SVA) of the trace display (ie, subjective assessment of the parallel course of the segmental traces) and by calculating the synchrony time index ($STI\varepsilon_R$), defined as the difference in $t\varepsilon_R$ from the earliest to the latest segment.[32] In addition to SVA, cut-off values ($STI\varepsilon_R$ higher than the 75, 90, and 95% percentile, respectively, of all measured $STI\varepsilon_R$ at the target HR) were also used to define dyssynchrony.

Finally, the motion of each segment was classified as normokinetic (segmental peak strain between 65 and 135% of the median peak strain of all 6 segments), hypokinetic (segmental peak strain $<65\%$ of the median), dyskinetic (segmental peak strain in opposite direction to the majority of segments, ie, negative ε_R or positive ε_L), or akinetic (segmental peak strain $<5\%$ of the median).[33]

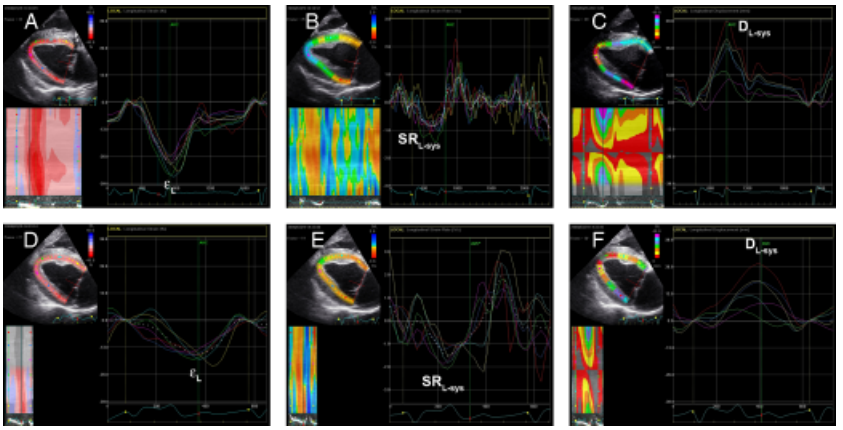

Fig 2. Two-dimensional speckle tracking (2DST) analyses of the left ventricle in long-axis recordings. Trace screens of the 2DST software are shown (for details see Fig 1). (**A**) Longitudinal strain at baseline. (**B**) Longitudinal strain rate at baseline. (**C**) Longitudinal displacement at baseline. (**D**) Longitudinal strain at HR_{120}. (**E**) Longitudinal strain rate at HR_{120}. (**F**) Longitudinal displacement at HR_{120}; ε_L, longitudinal peak strain; SR_{L-sys}, longitudinal peak systolic strain rate; D_{L-sys}, longitudinal peak systolic displacement.

Pulsed-wave TDI measurements and calculations were performed as described previously.[23] The following variables were measured to assess LV systolic function: Isovolumic contraction velocity (S_I), ejection velocity (S_m), pre-ejection period (PEP), isovolumic contraction time (IVCT), ejection time (ET), PEP-to-ET ratio (PEP/ET), and IVCT-to-ET ratio (IVCT/ET). For assessment of LV diastolic function, the following variables were measured: Isovolumic relaxation velocity (E_I), early-diastolic velocity (E_m), late-diastolic radial wall motion velocity (A_m), isovolumic relaxation time (IVRT), and E_m-to-A_m ratio (E_m/A_m). The index of myocardial performance (IMP, Tei index) was calculated as IMP = (IVCT + IVRT) / ET. For some of the PW TDI variables, triplicate measurements were not possible because of inability to clearly identify the respective velocity waves on the available recordings. The affected data points were reported as missing. No statistical analyses were performed for E_m, A_m, and the derived indices because of the fusion of E_m and A_m at higher HR and the large number of missing values. When the E_m velocity exceeded the lower limit of the velocity scale (−50 cm/s), a value of −50 cm/s was set and used for further calculations.

Statistics

All statistical and graphical analyses were performed with standard computer software.[e,f,g] Graphical presentation of the summarized data were achieved using box-and-whisker diagrams, with the line near the middle of the box indicating the median, the top and the bottom of the box indicating the upper and lower quartile, and the whiskers indicating the smallest and largest observations, respectively. For indices of LV dimensions and indices of global LV function, 1-way repeated-measures analysis of variance (ANOVA) was used to compare baseline and postexercise measurements. For 2DST indices of segmental LV function, 2-way repeated-measures ANOVA was used to detect differences between segments and HR (ie, between baseline and postexercise measurements). When the *F*-test indicated significant differences, all pairwise multiple comparisons were performed by the Holm-Sidak posthoc test. Valitity of the normality assumption was confirmed by assessment of normal probability plots of the residuals. The level of significance was $P = .05$.

Results

Feasibility and Quality of Recordings

Echocardiographic analyses were feasible in all 5 horses and during all 3 runs. In 4 horses, the HR dropped below 100 minute^{-1} within 128 ± 32 seconds (1st run 132 ± 28 seconds, 2nd run 116 ± 20 seconds, 3rd run 132 ± 53 seconds) after stopping the treadmill. In 1 horse, the HR dropped below 95 minute^{-1} within 25 ± 8 seconds (1st run 15 seconds, 2nd and 3rd run 30 seconds); therefore, no recordings were available for this horse at HR_{120}, HR_{110}, and HR_{100} (2D LAX and PW TDI only). In another horse, no PW TDI recordings were available at HR_{80} because the HR had not dropped below 85 minute^{-1} within 5 minutes after cessation of exercise.

2D and AMM Indices of LV Dimensions and Systolic LV Function

The results are summarized in Tables 1 and 2. The LVIVs was significantly increased during all postexercise

Table 1. Indices of left-ventricular dimensions measured using AMM and 2DE.

Variables	Units	Baseline	HR_{120}	HR_{110}	HR_{100}	HR_{90}	HR_{80}	*P* value (*F*-test)
AMM		(*n* = 5)	(*n* = 4)	(*n* = 4)	(*n* = 5)	(*n* = 5)	(*n* = 5)	
Measured HR	min^{-1}	36 ± 12	118 ± 1	108 ± 2	99 ± 2	90 ± 1	80 ± 2	—
IVSd	cm	3.2 ± 0.2	3.3 ± 0.5	3.4 ± 0.2	3.4 ± 0.2	3.3 ± 0.2	3.3 ± 0.2	.715
IVSs	cm	4.9 ± 0.2	4.8 ± 0.2	4.9 ± 0.1	5.2 ± 0.3	4.9 ± 0.2	5.0 ± 0.4	.143
LVIDd	cm	11.7 ± 1.0	10.7 ± 1.0	11.0 ± 0.8	11.1 ± 0.8	11.2 ± 0.9	11.1 ± 0.8	.060
LVIDs	cm	7.0 ± 1.1	6.3 ± 0.7	6.5 ± 0.6	6.5 ± 0.7	6.8 ± 0.8	6.9 ± 0.9	.179
LVFWd	cm	2.6 ± 0.5	2.4 ± 0.3	2.3 ± 0.2	2.3 ± 0.3	2.4 ± 0.2	2.4 ± 0.2	.125
LVFWs	cm	4.5 ± 0.5	4.6 ± 0.1	4.4 ± 0.2	4.5 ± 0.2	4.3 ± 0.3	4.2 ± 0.4	.034[a]
MWTd	cm	2.9 ± 0.3	2.8 ± 0.1	2.8 ± 0.1	2.8 ± 0.1	2.8 ± 0.2	2.8 ± 0.1	.850
MWTs	cm	4.7 ± 0.3	4.7 ± 0.1	4.6 ± 0.1	4.8 ± 0.2	4.6 ± 0.2	4.6 ± 0.3	.140
RWTd	—	0.50 ± 0.06	0.53 ± 0.04	0.52 ± 0.04	0.51 ± 0.04	0.51 ± 0.03	0.51 ± 0.03	.453
2D SAX		(*n* = 5)	(*n* = 4)	(*n* = 4)	(*n* = 5)	(*n* = 5)	(*n* = 5)	
Measured HR	min^{-1}	36 ± 12	118 ± 1	108 ± 2	99 ± 2	90 ± 1	80 ± 2	—
LVIAd	cm^2	101.8 ± 17.8	89.3 ± 21.1	90.6 ± 17.2	90.2 ± 16.4	91.9 ± 12.8	91.8 ± 11.6	.169
LVIAs	cm^2	32.8 ± 10.6	31.5 ± 9.7	33.2 ± 7.4	33.8 ± 6.4	34.9 ± 6.2	37.3 ± 10.0	.610
LVMAd	cm^2	107.2 ± 8.9	103.5 ± 13.3	101.6 ± 4.1	107.9 ± 4.1	105.1 ± 9.1	103.7 ± 7.9	.933
LVMAs	cm^2	148.3 ± 6.5	143.0 ± 11.0	140.1 ± 7.4	145.2 ± 5.9	145.7 ± 9.0	145.0 ± 6.8	.810
MWT_Ad	cm	2.5 ± 0.1	2.5 ± 0.2	2.5 ± 0.2	2.6 ± 0.2	2.5 ± 0.1	2.5 ± 0.1	.732
MWT_As	cm	4.4 ± 0.2	4.3 ± 0.2	4.2 ± 0.3	4.3 ± 0.2	4.2 ± 0.2	4.2 ± 0.3	.395
RWT_Ad	—	0.44 ± 0.05	0.48 ± 0.06	0.47 ± 0.09	0.49 ± 0.09	0.47 ± 0.04	0.46 ± 0.03	.207
2D LAX		(*n* = 5)	(*n* = 4)	(*n* = 4)	(*n* = 4)	(*n* = 5)	(*n* = 5)	
Measured HR	min^{-1}	35 ± 4	119 ± 2	110 ± 2	99 ± 1	88 ± 1	79 ± 2	—
LVIVd	cm^3	1,287.6 ± 229.3	1,127.9 ± 84.2	1,132.5 ± 190.9	1,204.4 ± 212.4	1,338.2 ± 272.8	1,354.6 ± 218.0	.057
LVIVs	cm^3	336.6 ± 87.3	429.8 ± 122.9[B]	394.4 ± 122.0[B]	431.8 ± 131.4[B]	460.7 ± 124.6[B]	445.1 ± 116.6[B]	< .001

Measurements are reported as mean ± SD.

[B] Significantly different from baseline (Holm-Sidak posthoc test).

[a]Variable for which the *F*-test indicated significant differences between groups that could not be substantiated by posthoc testing for multiple comparisons.

Table 2. Indices of left-ventricular systolic function measured using AMM and 2DE.

Variables	Units	Baseline	HR_{120}	HR_{110}	HR_{100}	HR_{90}	HR_{80}	*P* value (*F*-test)
AMM		($n = 5$)	($n = 4$)	($n = 4$)	($n = 5$)	($n = 5$)	($n = 5$)	
Measured HR	min^{-1}	36 ± 12	118 ± 1	108 ± 2	99 ± 2	90 ± 1	80 ± 2	—
FS	%	40.7 ± 4.3	41.3 ± 1.4	40.6 ± 2.5	42.1 ± 2.3	39.8 ± 4.1	38.7 ± 3.6	.365
2D SAX		($n = 5$)	($n = 4$)	($n = 4$)	($n = 5$)	($n = 5$)	($n = 5$)	
Measured HR	min^{-1}	36 ± 12	118 ± 1	108 ± 2	99 ± 2	90 ± 1	80 ± 2	—
EMS	ms	519 ± 32	$314 \pm 20^{B,80,90}$	$346 \pm 23^{B,80}$	$343 \pm 32^{B,80,90}$	377 ± 31^{B}	402 ± 31^{B}	< .001
LV FAC	%	68.5 ± 6.2	65.1 ± 2.7	63.4 ± 1.6	62.5 ± 2.2	62.1 ± 2.7	59.9 ± 6.2^{B}	.025
MWT_A FC	%	79.8 ± 10.3	68.4 ± 3.7	73.5 ± 7.0	67.3 ± 7.5	68.0 ± 3.4	66.5 ± 7.9	.027[a]
MWT_A FC/EMS	s^{-1}	1.53 ± 0.20	$2.18 \pm 0.19^{B,80,90}$	$2.13 \pm 0.20^{B,80}$	$1.96 \pm 0.13^{B,80}$	1.81 ± 0.13	1.66 ± 0.18	< .001
LVMA FC	%	40.7 ± 6.8	31.7 ± 4.4	40.9 ± 8.1	36.4 ± 7.4	37.5 ± 5.4	38.9 ± 6.7	.162
LVMA FC/EMS	s^{-1}	0.79 ± 0.13	1.00 ± 0.09	1.18 ± 0.24^{B}	1.06 ± 0.17	1.00 ± 0.16	0.97 ± 0.15	.016
2D LAX		($n = 5$)	($n = 4$)	($n = 4$)	($n = 4$)	($n = 5$)	($n = 5$)	
Measured HR	min^{-1}	35 ± 4	119 ± 2	110 ± 2	99 ± 1	88 ± 1	79 ± 2	—
SV	mL	951 ± 159	$698 \pm 109^{B,80}$	738 ± 107^{B}	774 ± 100	877 ± 170	910 ± 115	.005
CO	$L\ min^{-1}$	32.9 ± 3.2	82.9 ± 13.5^{B}	81.0 ± 11.2^{B}	76.2 ± 10.0^{B}	77.4 ± 14.2^{B}	71.9 ± 7.2^{B}	< .001
EF	%	74.0 ± 3.5	62.3 ± 7.6^{B}	65.6 ± 6.8^{B}	64.7 ± 5.8^{B}	65.7 ± 5.5^{B}	67.6 ± 4.5^{B}	< .001

Measurements are reported as mean ± SD.
[B]Significantly different from baseline (Holm-Sidak posthoc test).
[80]Significantly different from HR 80 (Holm-Sidak posthoc test).
[90] Significantly different from HR 90 (Holm-Sidak posthoc test).
[a]Variable for which the *F*-test indicated significant differences between groups that could not be substantiated by posthoc testing for multiple comparisons.

periods compared with baseline. The LVIVd and the LVIDd showed a slight, but statistically not significant decrease postexercise. None of the other indices of LV dimensions changed significantly after exercise compared with baseline. Among the indices of LV systolic function, MWT_A FC/EMS and LVMA FC/EMS increased significantly, whereas SV and EF decreased significantly postexercise compared with baseline. Despite the decrease in SV, CO increased significantly at higher HR postexercise. The LV FAC was significantly decreased at HR_{80} only, and FS did not change significantly postexercise.

2D Speckle Tracking

Generally, when systolic 2DST was approved by the software, it also appeared accurate when assessed visually by the operator. In rare cases, the endocardial border was not tracked accurately during the last 1 or 2 frames of systole. This was observed in 4 different segments in 4 cardiac cycles of 3 horses in SAX. The basal lateral segment was affected in 5 cycles of the same 3 horses in LAX. Hence, 9 out of a total of 162 analyzed cycles (5.6%) were affected. Because tracking in the affected segments appeared sufficient during the remainder of the cycle and because the software approved the tracking quality, these segments and cycles were not precluded from analyses.

2DST Indices of Systolic LV Function Obtained from SAX Recordings (Fig 1A–F)

Of the 15 cardiac cycles available from the recordings obtained at rest, all were analyzable by 2DST, and all segments were judged as normokinetic. Out of the 69 available cardiac cycles that were obtained after exercise, all segments were analyzable by 2DST. Three segments in 2 horses were judged as hypokinetic, but none of the segments was consistently judged hypokinetic on all 3 recordings (Table 3). No segment showed akinesia or dyskinesia. Based on SVA of the trace displays, 6 out of 84 recordings were judged dyssynchronous, affecting 3 horses (Table 4). None of the horses showed dyssynchrony by SVA at baseline and none of the horses showed consistent dyssynchrony by SVA on all 3 recordings at any time point. When using the percentiles of the measured $STI\varepsilon_R$ as cut-off values, between 0 (cut-off set at the 95% percentile) and 17 recordings (cut-off set at the 75% percentile) were judged as dyssynchronous, affecting maximally 4 horses. The results of the quantitative 2DST analysis obtained from SAX recordings are summarized in Figure 3. Comparison between segments did not reveal significant differences for any of the 2DST indices. Comparison between baseline and postexercise periods showed significant differences: ε_R, $t\varepsilon_R$, and D_{R-sys} were significantly decreased at all postexercise periods compared with baseline. SR_{R-sys} was significantly increased compared with baseline at HR_{120}, HR_{110}, and HR_{100}.

2DST Indices of Systolic LV Function Obtained from LAX Recordings (Fig 2A–F)

From the 78 cardiac cycles available for analyses, 14 out of 468 segments had to be excluded because of inadequate tracking (Table 3). On the 15 cardiac cycles analyzed at rest, 2 segments were judged as hypokinetic in 2 horses. On the 63 cardiac cycles analyzed after exer-

Table 3. 2DST analysis. Summary of excluded segments and hypokinetic segments.

Segment / Horse	Baseline					HR_{120}					HR_{110}					HR_{100}					HR_{90}					HR_{80}				
	1	2	3	4	5	1	2	3	4	5	1	2	3	4	5	1	2	3	4	5	1	2	3	4	5	1	2	3	4	5
SAX																														
Ant														H_1																
Sept																														
Ant																			H_2											
Lat																														
Post																														
Inf																														
Sept							H_1																							
LAX																														
Ap Lat								H_1																		E_2	E_1			
Ap Sept								E_1																		E_1	E_1			
Mid Lat						H_1		H_1	H_2										H_1					H_2			H_2		
Mid Sept		H_1			H_1			H_1			H_1																			
Bas Lat										H_1	H_1			H_1										H_2		H_1	E_1			
Bas Sept		E_2	E_2	E_1																		E_1						E_1		

H, hypokinetic (segmental peak strain $<65\%$ of the median peak strain of all 6 segments); E, segment excluded due to inadequate tracking; 1, seen in one recording; 2, seen in two recordings.

cise, 18 segments were judged as hypokinetic. All 5 horses were affected, but none of the segments was consistently judged hypokinetic on all 3 recordings in any of the horses (Table 3). No segment showed dyskinesia or akinesia. The results of the quantitative 2DST analysis obtained from LAX recordings are summarized in Figure 4A–D. Shortly, in all segments except bas Sept, ε_L was significantly decreased at HR_{120} and HR_{110} compared with baseline. There were no significant differences within each time period in ε_L between apical, mid, and basal segments, except for the basal segments at HR_{90} and HR_{80}; no distinct gradient from base to apex could be demonstrated. In all segments, SR_{L-sys} was significantly increased at all postexercise periods compared with baseline. A small but significant difference in SR_{L-sys} was seen between the apical segments, whereas no significant differences were seen between mid segments and basal segments. In all except the apical segments, D_{L-sys} was significantly decreased at HR_{120}, HR_{110}, HR_{100}, and HR_{90} compared with baseline. A distinct basal-to-apical gradient was seen in D_{L-sys}. The $t\varepsilon_L$ significantly decreased at all postexercise HR compared with baseline. Peak longitudinal strain occurred significantly earlier in the apical segments compared with the mid septal, basal septal, and basal lateral segments.

PW TDI Indices of LV Function

The results are summarized in Table 5. At baseline, the LV radial wall motion velocity profile appeared very consistently in all horses, as described elsewhere,[23] and triplicate measurement was possible for all variables in all horses. This was in contrast to postexercise recordings, where velocity waves were not always clearly identifiable. Only in 1 horse, all waves were identifiable at all HR. Only S_m and E_m were identifiable in all horses

Table 4. Synchrony time index and assessment of dyssynchrony based on subjective visual assessment (SVA) and using different quantitative cut-off values.

$STI\varepsilon_R$ (ms)	Baseline	HR_{120}	HR_{110}	HR_{100}	HR_{90}	HR_{80}
Minimum	0	0	0	0	18	0
Median	19	0	9	18	19	19
75% perc.	111	32	84	37	37	74
90% perc.	119	142	106	81	82	101
95% perc.	130	148	111	92	93	112
Maximum	130	148	111	92	93	112

Assessment of dyssynchrony																														
Horse	1	2	3	4	5	1	2	3	4	5	1	2	3	4	5	1	2	3	4	5	1	2	3	4	5	1	2	3	4	5
SVA										2×			1×				2×											1×		
> 75% perc.			1×	1×				1×		2×			1×		2×		2×			1×				3×			1×		2×
> 90% perc.				1×						1×			1×				1×							1×					1×
> 95% perc.																														

SVA, segments were judged as dyssynchronous based on subjective visual assessment; > 75% perc., values greater than the 75% percentile of all measured $STI\varepsilon_R$ were judged as dyssynchronous; > 90% perc., values greater than the 90% percentile of all measured $STI\varepsilon_R$ were judged as dyssynchronous; > 95% perc., values greater than the 95% percentile of all measured $STI\varepsilon_R$ were judged as dyssynchronous.

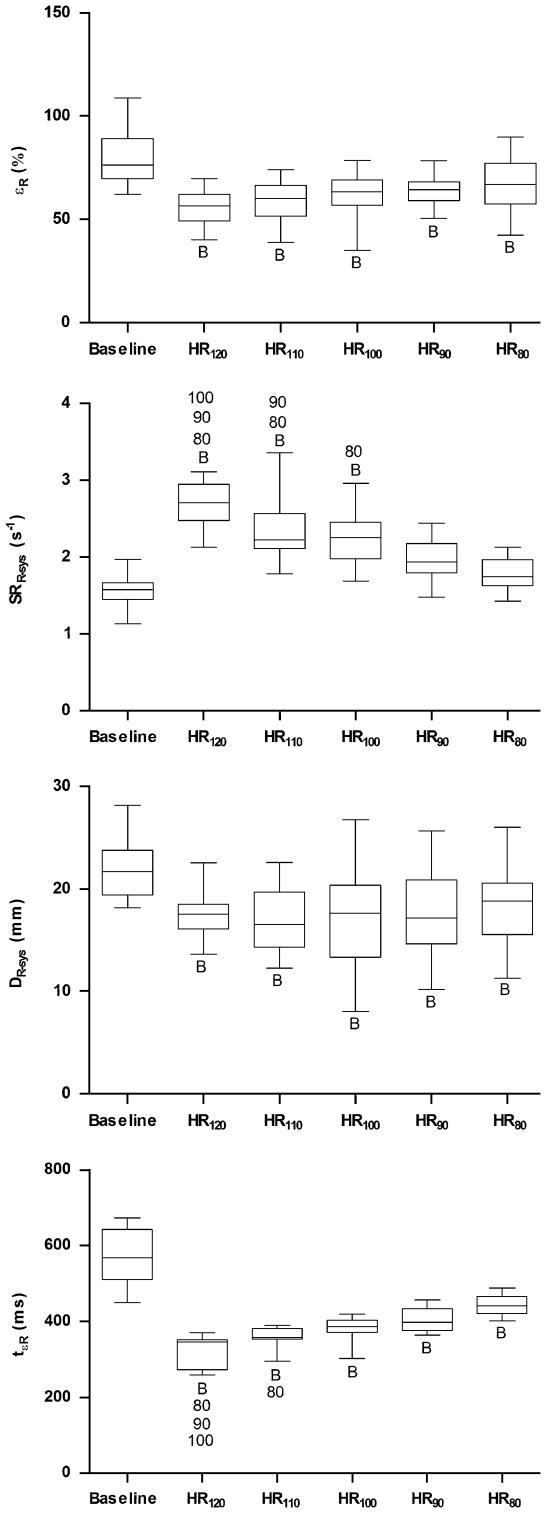

Fig 3. Results from 2D speckle tracking (2DST) analyses of left-ventricular short-axis recordings. No significant differences where identified between segments. Therefore, segmental data are pooled at each time period for graphical presentation. Significant differences between time points are marked as follows: B, significantly different from Baseline; 80, significantly different from HR_{80}; 90, significantly different from HR_{90}; 100, significantly different from HR_{100}; ε_R, radial peak strain; SR_{R-sys}, radial peak systolic strain rate; D_{R-sys}, radial peak systolic displacement; $t\varepsilon_R$, time to radial peak strain.

throughout all HR. In all but 1 horse, A_m was fused with E_m at HR_{120} and at HR_{110}. E_m and (E_m + A_m), respectively, exceeded the velocity scale in all horses at HR_{120} and HR_{110}, and in all but 1 horse at HR_{100}. Identification of A_m was not possible in 37 out of 63 postexercise cardiac cycles (59%). In only 2 horses, S_1 and E_1 were identifiable in all cardiac cycles recorded after exercise; reliable identification was not possible in the remaining horses for S_1 in 17/63 cycles (27%) and for E_1 in 14/63 cycles (22%).

Discussion

The results of this study show that quantitative analysis of stress echocardiograms in horses after high-speed treadmill exercise is feasible using 2DE, AMM, and 2DST, while the application of TDI is technically difficult and inaccurate. Some of the investigated echocardiographic indices are able to detect consistent alterations in LV function after cessation of exercise.

The availability of accurate and reliable methods for assessment of global and regional cardiac function is crucial to study the clinical value of stress echocardiography in horses. Currently, routine imaging methods used for assessment of global LV function rely on 2DE, M-mode, and flow Doppler methods.[16–19,34] Most commonly, ejection phase indices are calculated from one-dimensional M-mode measurements of LV dimensions, with the FS being the only index routinely used in horses.[16–18] However, reliance on the FS as a single index of LV systolic function is problematic, because it represents the shortening of the LV in a single dimension, disregarding the fact that the LV contracts in all three dimensions. Also, it lacks accuracy in the presence of ventricular dyssynchrony, regional wall motion abnormalities, or malposition of the cursor line. It is therefore not surprising that there is disagreement in the current literature regarding the time course after treadmill exercise of LV FS and other conventional 2DE and M-mode indices in horses.[4,6,9,11] The results of this study revealed that AMM and—for most instances—area-based indices of LV dimensions and LV systolic function are generally not suitable to detect exercise-induced changes in LV function. Among the area-based indices, only MWT_A FC/EMS, reflecting myocardial deformation rate, increased significantly in the immediate postexercise period, mostly because of the observed shortening of EMS.

Volumetric estimates of LV size and function are considered more accurate and less affected by altered chamber geometry than linear indices.[35,36] The volumetric LV EF is a standard index of LV systolic function in humans. It is not commonly used in horses, mostly because many of the required imaging planes are difficult to obtain in large animals.[16] Furthermore, all volumetric indices are calculated based on geometrical assumptions and approximations, limiting their accuracy.[16–18] Despite these restrictions, the results of the current study suggest that volumetric estimates of LV dimensions and function obtained from LAX views are superior to linear and area-based SAX indices in identifying exercise-induced changes of LV function in healthy horses after treadmill

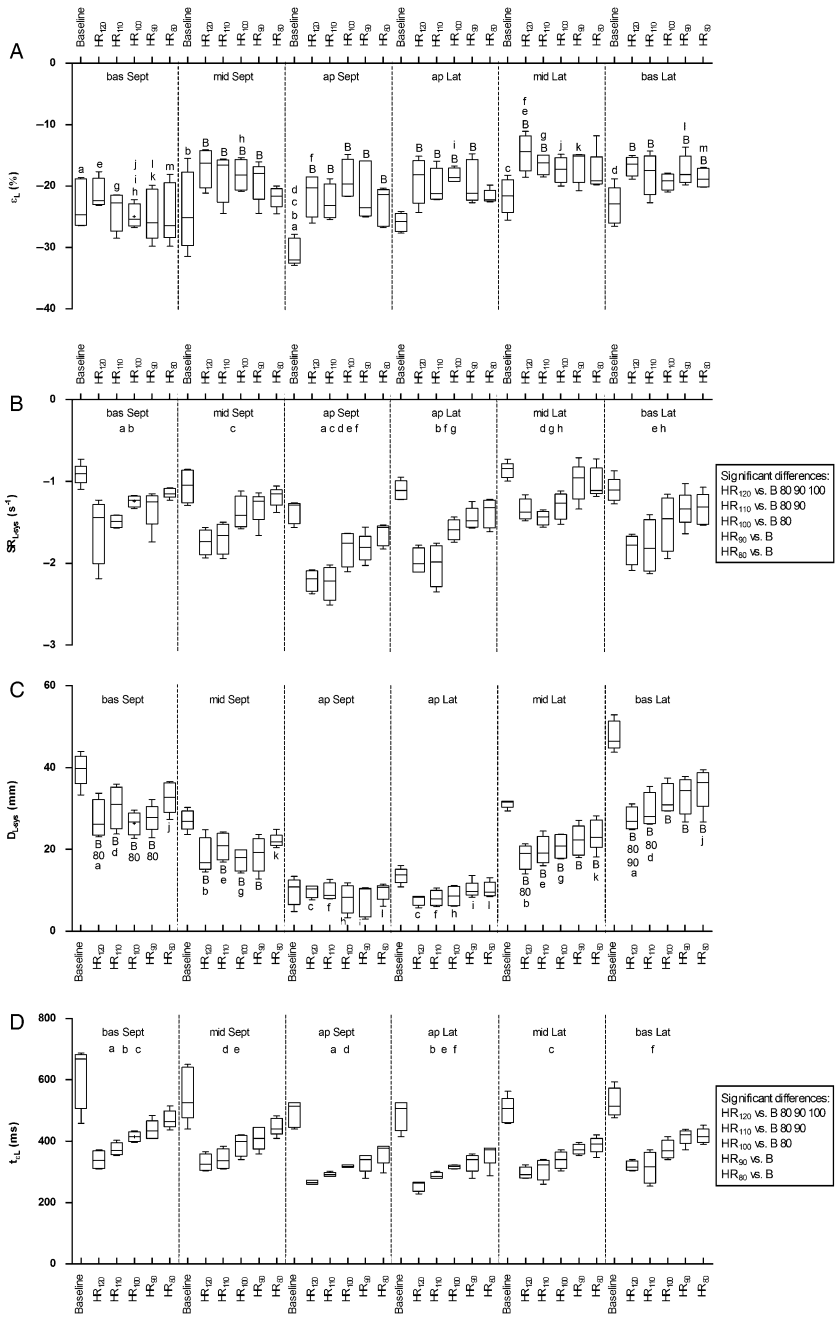

Fig 4. Results from 2D speckle tracking (2DST) analyses of left-ventricular long-axis recordings. (**A**) Longitudinal peak strain (ε_L). There was a statistically significant interaction between segment and heart rate (HR) ($P = .01$). Significant differences between HRs within segments are marked as follows: B, significantly different from Baseline; 80, significantly different from HR_{80}; 90, significantly different from HR_{90}; 100, significantly different from HR_{100}. Within each HR, segments marked with the same letter *are* significantly different from each other. (**B**) Longitudinal peak systolic strain rate (SR_{L-sys}). The difference between segments ($P < .001$) and the difference between HRs ($P < .001$) were statistically significant, but there was no significant interaction between segment and HR ($P = .301$). Segments marked with the same letter *are* significantly different from each other. Significant differences between HRs are listed as described above. (**C**) Longitudinal peak systolic displacement (D_{L-sys}). There was a statistically significant interaction between segment and HR ($P < .001$). Significant differences between HRs within segments are marked as described above. Within each HR, segments marked with the same letter *are not* significantly different from each other. (**D**) Time to longitudinal peak strain ($t\varepsilon_L$). The difference between segments ($P < .001$) and the difference between HRs ($P < .001$) were statistically significant, but there was no significant interaction between segment and HR ($P = .161$). Segments marked with the same letter *are* significantly different from each other. Significant differences between HRs are listed as described above.

exercise. This can be explained by the large impact of ventricular length on volumetric LV estimates by Simpson's method. The results therefore indicate that systolic length of the LV increased after exercise (data not shown), concordant to the decrease of D_{L-sys} after exercise. These findings support the contention that LAX

Table 5. Indices of left-ventricular systolic and diastolic function using TDI.

Variables	Unit	Baseline	n	HR_{120}	n	HR_{110}	n	HR_{100}	n	HR_{90}	n	HR_{80}	n	*P* value (*F*-test)
Measured HR	min^{-1}	35 ± 5		120 ± 2		109 ± 1		99 ± 1		90 ± 1		80 ± 1		
Variables of systolic LV function														
S_l	cm/s	4.9 ± 2.4	5	9.9 ± 0.2	3	8.0 ± 3.6	4	7.4 ± 1.6	4	6.3 ± 1.7	5	5.2 ± 0.7	2	.083
S_m	cm/s	12.0 ± 2.0	5	20.8 ± 3.7[B,90]	4	17.8 ± 3.1[B]	4	16.3 ± 1.4	4	14.9 ± 3.8	5	15.3 ± 1.2	4	.002
IVCT	ms	60 ± 8	5	50 ± 20	3	46 ± 19	4	53 ± 18	4	53 ± 13	5	56 ± 19	2	.072
PEP	ms	102 ± 22	5	101 ± 13	4	98 ± 4	4	104 ± 6	4	100 ± 7	5	104 ± 13	4	.970
ET	ms	433 ± 28	5	200 ± 26[B,80,90]	4	234 ± 24[B,80]	4	249 ± 15[B,80]	4	274 ± 19[B,80]	5	329 ± 33[B]	4	< .001
PEP/ET	—	0.24 ± 0.04	5	0.52 ± 0.13[B,80,90]	4	0.43 ± 0.05[B]	4	0.42 ± 0.05[B]	4	0.37 ± 0.05[B]	5	0.32 ± 0.05	4	< .001
IVCT/ET	—	0.14 ± 0.02	5	0.27 ± 0.13	3	0.20 ± 0.06	4	0.21 ± 0.07	4	0.20 ± 0.06	5	0.18 ± 0.06	2	.056
Variables of diastolic LV function and left atrial function														
E_l	cm/s	7.0 ± 1.8	5	9.7 ± 4.5	3	7.3 ± 3.3	3	7.5 ± 1.8	4	7.1 ± 2.4	5	6.4 ± 1.7	3	.426
E_m	cm/s	33.7 ± 5.8	5	> 50[b]	1	> 50[b]	1	44.0 ± 10.4	3	40.5 ± 2.8	5	38.2 ± 6.4	4	ND
$E_m + A_m$	cm/s	—	—	> 50[b]	3	> 50[b]	3	> 50[b]	1	—	—	—	—	ND
IVRT	ms	49 ± 16	5	37 ± 8	3	46 ± 19	3	47 ± 16	4	49 ± 11	5	44 ± 9	3	.459
A_m	cm/s	12.5 ± 3.6	5	23	1	20.3	1	17.1 ± 6.5	3	16.7 ± 5.8	5	16.9 ± 1.7	3	ND
E_m/A_m	—	2.92 ± 0.92	5	2.20	1	2.50	1	2.69 ± 0.52	3	2.81 ± 1.35	5	2.47 ± 0.39	3	ND
Index of systolic and diastolic LV function														
IMP	—	0.26 ± 0.01	5	0.47 ± 0.18	3	0.35 ± 0.09	3	0.41 ± 0.11	4	0.38 ± 0.09	5	0.30 ± 0.09	2	.035[a]

Measurements are reported as mean ± SD.

ND, no statistical analyses performed.

[B] Significantly different from baseline (Holm-Sidak posthoc test).

[80] Significantly different from HR 80 (Holm-Sidak posthoc test).

[90] Significantly different from HR 90 (Holm-Sidak posthoc test).

[a]Variable for which the *F*-test indicated significant differences between groups that could not be substantiated by posthoc testing for multiple comparisons.

[b]Values exceeding the velocity scale.

motion of the LV is an important component of LV function[37] that undergoes dynamic changes during and after exercise, while adaptations in radial (SAX) motion only play a minor role.

The LVIVs increased and the SV and EF decreased significantly after exercise compared with baseline, whereas the CO, because of the high HR, increased significantly. Although these findings seem counterintuitive, they were similar to the results of a study in ponies, in which systolic shortening measured by ultrasonic crystals increased during exercise but was significantly reduced after exercise.[38] The slight but not significant decline in end-diastolic LV dimensions is suggestive of an exercise-induced decrease in ventricular filling, most likely related to the increase in HR that shortens diastolic ventricular filling time. This could explain the decrease in SV at higher HR.[39] Most likely, other factors related to rapidly changing autonomic input, preload, afterload, contractility and their complex interrelation also play a role during the immediate postexercise period.

Quantitative characterization of LV wall motion in horses has recently been investigated using tissue velocities by TDI[23] as well as strain and strain rate by 2DST.[32] The results of the current study showed that S_m and PEP/ET increased after exercise while ET decreased at higher HR because of the shortening of the ejection period. The significant increase in S_m is in accordance to studies in people, indicating an increase in LV systolic performance during and after exercise.[40–43] The significant increase in PEP/ET can be explained with the increase in HR and the slight but not significant decrease in preload (reflected by LVIVd).[16,44] None of the other TDI variables changed consistently and significantly after exercise. However, only S_m and E_m were identifiable in all horses and throughout all HR, while difficulties in identifying velocity waves at higher HR often precluded the measurement of S_l, E_l, IVRT, and IMP. The low number of measurements during isovolumic periods might be responsible for the inability to detect significant changes after exercise.

Assessment of diastolic LV function is difficult in horses. While 2DST is considered unreliable for assessment of radial LV diastolic wall motion,[32] TDI allows reliable assessment of diastolic LV wall motion in horses at rest.[23] The results of this study showed that, in agreement with previous studies in people,[42,43] both E_m and A_m by PW TDI increased after exercise. However, fusion of E_m and A_m waves[40,45] was seen at HR_{120} and HR_{110} and therefore prevented their measurement in the majority of horses. Furthermore, E_m and $E_m + A_m$, respectively, exceeded the maximum velocity scale at higher HR. The value of PW TDI for quantitative stress echocardiography is therefore highly limited. If to be used at all, its use should be limited to the measurement of systolic S_m and PEP/ET. It is unknown if color TDI (cTDI) would have offered some additional value over PW TDI. In a previous study in horses, cTDI did not provide substantial advantages over PW TDI for analysis

of radial LV wall motion velocities and it was less reliable, particularly pertaining to strain and strain rate analyses.[23]

Wall motion analysis by 2DST is considered superior to TDI because of its independence of the angle of interrogation and the ability to assess segmental myocardial motion in two dimensions simultaneously.[24,31,32,46] The results of this study showed that both ε_R and ε_L by 2DST decreased after exercise. This finding is in agreement with the decrease in SV and EF, supporting the contention that strain is an analog of regional EF and largely reflects changes in SV.[25,47,48] The SR_{R-sys} and the SR_{L-sys} by 2DST as well as the corresponding MWT_A FC/EMS by 2DE increased significantly after exercise, most likely reflecting an increase in regional and global myocardial contractility.[25,47,48] Overall, the results of this study suggest that 2DST derived strain and strain rate are more sensitive and more reliable than 2DE and TDI measurements for assessment of stress-induced changes in myocardial function.

Analysis of myocardial motion by 2DST provides interesting insights into the mechanics of LV contraction. The basal-to-apical gradient seen in D_{L-sys} again emphasizes the importance of longitudinal LV function, indicating that during LV systole the apex remains relatively stationary while the atrioventricular plane moves toward the apex.[46,49] The decrease in D_{R-sys} and—except for apical segments—in D_{L-sys} postexercise is consistent with the concurrent drop in ε_R, ε_L, SV, and EF. A partly significant, but not very distinct apical-to-basal ε_L gradient was seen at rest but not after exercise. An apical-to-basal decrease in ε_L has also been shown in humans,[50–52] pigs,[53] and goats,[54] although in other studies strain was evenly distributed throughout the myocardium.[46] Assessment of $t\varepsilon_L$ indicated that, in agreement with recently published findings in people,[51] the peak ε_L occurred significantly earlier in the apex compared with mid septal and basal septal segments. This finding is likely related to the fact that in mammalian hearts, electrical activation of the ventricles begins near the apical septum and spreads rapidly toward the base.[53–56] Independent of HR, the SR_{L-sys} was highest in the apical septal segment compared with all other segments, suggesting a slight apical-to-basal SR_{L-sys} gradient, similar to findings in pigs[53] and goats.[54] Conversely, studies in people did not show significant differences in SR_{L-sys} between segments.[46,52]

Evaluation of regional ventricular function can provide important diagnostic and prognostic information on human patients with coronary artery disease,[24,25,27] but the clinical relevance of regional wall motion analysis in horses is unknown. Therefore, there is a need to investigate novel echocardiographic methods to better quantify myocardial wall motion abnormalities that could be suggestive of occult myocardial disorders. Echocardiographic assessment of regional myocardial function has traditionally been achieved by combining visual analysis of endocardial motion with the measurement of wall thickening and thinning from 2D images.[17–19] Wall motion can also be evaluated semiquantitatively by generation of a wall motion score index.[19] However, these methods are largely subjective.[57] The low interobserver agreement[58,59] and the potential for failure to identify areas of subtle abnormalities make these methods relatively inaccurate and unreliable.

Ischemic regions are characterized by a decrease in systolic velocities,[40,41,60] a decrease in systolic strain and strain rate,[61,62] and a delayed onset of relaxation.[63] The 2DST technology provides an objective way to identify hypokinetic and akinetic myocardial segments and to quantify the degree of wall motion anomalies.[24,30,31] However, to our knowledge there are no established cut-off values to differentiate normokinetic from hypokinetic and akinetic segments. The definition we used in this study was chosen based on a human study using MRI as the gold standard for identification of hypokinesia and akinesia.[33] By our definition, a relatively large number of segments were judged as being hypokinetic. All 5 horses were affected, but none of the segments was consistently judged as being hypokinetic on all 3 recordings. In our opinion, the high number of hypokinetic segments detected in this population of healthy athletic horses is likely to be a result of artifacts related to the image quality or to the tracking algorithm rather than true, clinically relevant hypokinesia. We propose that hypokinesia should only be diagnosed when the same segment is judged as being hypokinetic in all 3 recordings of the same HR and when the affected segment is the same throughout the postexercise period.

Although stress echocardiography is commonly used to detect ventricular dyssynchrony in people, there is currently no single index that is considered optimal for assessment of dyssynchrony.[64] Evaluation of dyssynchrony by 2DST can be achieved by visual assessment of the graphical display of segmental myocardial motion and by calculating a variety of synchrony indices.[32,65,66] In this study, we assessed synchrony based on SVA of the trace display as well as by using different percentiles of all calculated $STI\varepsilon_R$ as cut-off values.[32] Although not formally tested, agreement between SVA and the more objective percentile-based method was obviously poor. Some of the recordings that were judged as dyssynchronous when using a cut-off value higher than the 75 and the 90% percentile, respectively, were judged as synchronous by SVA. Based on these results and the previously reported poor reliability of the $STI\varepsilon_R$,[32] we cannot recommend the use of the $STI\varepsilon_R$ as a single index of myocardial dyssynchrony in horses.

Further studies in a larger population including healthy horses and horses with myocardial disease will be necessary to elaborate a clinically applicable and objective definition for hypokinesia and akinesia and to investigate the best diagnostic approach to detect ventricular dyssynchrony on horses. In any case, subjective confirmation of adequate tracking by the observer and SVA of the 2DST trace display will likely remain important in the assessment of regional wall motion abnormalities in horses.

We were able to show that some of the echocardiographic indices of LV function obtained within the first 5 minutes after high-speed treadmill exercise are highly variable and largely depend on HR. Sandersen et al[9]

showed that most of the linear M-mode variables of LV size and function measured during stress echocardiography did not differ significantly from baseline at HR below 100 minute^{-1}. These findings are in agreement with the results of this study in healthy horses, demonstrating that all of the potentially useful indices of LV systolic function, in particular ε_R, ε_L, SR_{R-sys}, and SR_{L-sys} as well as MWT_A FC/EMS, S_m, and PEP/ET, showed consistent and significant increases compared with baseline at HR above 100 minute^{-1}. Whether horses with stress-induced myocardial dysfunction show abnormalities in a wider range of HR will have to be investigated in future studies. In any case, the results suggest that the instantaneous HR needs to be considered when assessing quantitative stress echocardiographic measurements in individual horses.

The relatively small study population certainly needs to be listed as a limitation of this study, especially because values for higher HR could not be obtained in 1 horse. However, it was not possible to recruit a larger number of healthy horses in athletic condition that would have been allowed to undergo 3 consecutive exercise tests within a reasonable time frame. Nonetheless, the data still allowed identifying a number of echocardiographic indices that might prove useful for quantitative assessment of stress echocardiograms in horses.

Although the results were interpreted and discussed all together, it needs to be emphasized that the SAX 2DE recordings, the LAX 2DE recordings, and the TDI recordings were acquired on 3 separate occasions. This may be considered a 2nd limitation of the study. However, the goal of this study was to observe changes over time in a variety of echocardiographic indices postexercise and to relate the measurements to HR. In order to acquire complete datasets for each view and for each echocardiographic modality, including a minimum of 3 cardiac cycles at each target HR, it was necessary to obtain the recordings on 3 separate occasions.

Further limitations are of technical nature. Acquisition and analysis of high-quality recordings require extensive operator training as well as high-end echocardiographic equipment with digital raw-data storage and off-line postprocessing capabilities. On postexercise recordings, excessive translational motion of the heart, poor acoustic coupling, and a variety of artifacts sometimes prevent accurate identification of the myocardial border, particularly on the apex and on the septal base in the LAX plane. Generally, 2DST analysis of LAX recordings was more difficult than analyzing SAX images, and achieving adequate tracking of LAX recordings often required several attempts or was not possible (leading to exclusion of segments from further analyses), whereas tracking of SAX segments mostly was adequate at the first try. In rare cases, end-systolic tracking appeared slightly inaccurate, although the software approved the quality of the tracking. This might have been related to the rather low frame rate that was insufficient to resolve the high maximum wall motion velocities occurring at high HR in some segments. Theoretically, this phenomenon may lead to an underestimation of peak-systolic strain, strain rate, or displacement. However, because of the low number of affected segments, we do not anticipate a significant influence on the final results.

In conclusion, we were able to show that stress echocardiographic recordings can be quantitatively analyzed by conventional 2DE as well as novel 2DST methods. Volumetric estimates of SV and EF by 2DE, MWT_A FC/EMS by 2DE, as well as radial and longitudinal strain and strain rate by 2DST can be useful for quantitative stress-echocardiographic assessment of global and regional LV systolic function in horses, whereas linear and most area-based 2DE indices do not allow detecting significant and consistent stress-induced changes in LV function. Pulsed-wave TDI provides little additional information and its use is limited by poor image quality and unreliable identification of velocity waves at high HR. The results of this study further indicate that quantitative echocardiographic indices of LV function must be evaluated in view of the instantaneous HR. The detection of stress-induced hypokinesia, akinesia, and dyssynchrony in diseased horses requires additional investigations.

The results of this study provide a sound basis for future investigations into the clinical value of stress echocardiography in horses. It remains to be shown in a larger study population which of the echocardiographic indices will be clinically useful for quantitative assessment of LV function during stress echocardiography in horses with cardiac disease.

Footnotes

[a] EchoPAC Software Version 6.1.2, GE Medical Systems, Milwaukee WI
[b] Mustang 2200, Graber AG, CH-5615 Fahrwangen, Switzerland
[c] GE Vivid 7 Dimension, BTO6, GE Medical Systems
[d] M4S Phased Array Transducer, GE Medical Systems
[e] Microsoft Office Excel 2003, Microsoft Corporation, Redmond, WA
[f] SigmaStat v3.5, SPSS Inc, Chicago, IL
[g] GraphPad Prism v5.00 for Windows, GraphPad Software, San Diego, CA

Acknowledgments

The authors acknowledge Dagmar S. Trachsel and Katja von Peinen for their assistance with exercise testing.

References

1. Martin BB, Reef VB, Parente EJ, et al. Causes of poor performance of horses during training, racing, or showing: 348 cases (1992-1996). J Am Vet Med Assoc 2000;216:554–558.

2. Kriz NG, Hodgson DR, Rose RJ. Prevalence and clinical importance of heart murmurs in racehorses. J Am Vet Med Assoc 2000;216:1441–1445.

3. Patteson MW, Cripps PJ. A survey of cardiac auscultatory findings in horses. Equine Vet J 1993;25:409–415.

4. Reef VB. Stress echocardiography and its role in performance assessment. Vet Clin North Am Equine Pract 2001;17:179–189.

5. Bonagura JD, Reef V. Disorders of the cardiovascular system. In: Reed S, Bayly W, Sellon D, eds. Equine Internal Medicine, 2nd ed. Philadelphia, PA: WB Saunders; 2004:355–460.

6. Sandersen C. Stress echocardiography in horses—a review. Pferdeheilkunde 2006;22:609–617.

7. Frye MA, Bright JM, Dargatz DA, et al. A comparison of dobutamine infusion to exercise as a cardiac stress test in healthy horses. J Vet Intern Med 2003;17:58–64.

8. Sandersen CF, Detilleux J, Delguste C, et al. Atropine reduces dobutamine-induced side effects in ponies undergoing a pharmacological stress protocol. Equine Vet J 2005;37:128–132.

9. Sandersen C, Detilleux J, Art T, et al. Exercise and pharmacological stress echocardiography in healthy horses. Equine Vet J 2006;(Suppl);36:159–162.

10. Marr CM, Bright JM, Marlin DJ, et al. Pre- and post exercise echocardiography in horses performing treadmill exercise in cool and hot/humid conditions. Equine Vet J Suppl 1999;30:131–136.

11. Durando MM, Slack J, Reef VB, et al. Right ventricular pressure dynamics and stress echocardiography in pharmacological and exercise stress testing. Equine Vet J Suppl 2006;36:183–192.

12. Gehlen H, Marnette S, Rohn K, et al. Echocardiographic analysis of segmental left ventricular wall motion at rest and after exercise in horses with and without heart disease. J Equine Vet Sci 2005;25:468–479.

13. Sandersen CF, Detilleux J, de Moffarts B, et al. Effect of atropine-dobutamine stress test on left ventricular echocardiographic parameters in untrained warmblood horses. J Vet Intern Med 2006;20:575–580.

14. Grenacher PA, Schwarzwald CC. Assessment of left ventricular size and function in horses using anatomical M-mode echocardiography. J Vet Cardiol 2010, accepted.

15. Carerj S, Micari A, Trono A, et al. Anatomical M-mode: An old-new technique. Echocardiography 2003;20:357–361.

16. Boon J. Evaluation of size, function, hemodynamics. In: Boon JA, ed. Manual of Veterinary Echocardiography. Baltimore, MD: Williams & Wilkins; 1998:151–260.

17. Feigenbaum H, Armstrong W, Ryan T. Evaluation of systolic and diastolic function of the left ventricle. In: Feigenbaum H, Armstrong W, Ryan T, eds. Feigenbaum's Echocardiography, 6th ed. Philadelphia, PA: Lippincott Williams & Wilkins; 2005:138–180.

18. Otto C. 1Left and right ventricular systolic function. In: Otto C, ed. Textbook of Clinical Echocardiography, 3rd ed. Philadelphia, PA: Saunders; 2004:131–165.

19. Lang RM, Bierig M, Devereux RB, et al. Recommendations for chamber quantification: A report from the American Society of Echocardiography's Guidelines and Standards Committee and the Chamber Quantification Writing Group, developed in conjunction with the European Association of Echocardiography, a branch of the European Society of Cardiology. J Am Soc Echocardiogr 2005;18:1440–1463.

20. Schwarzwald CC, Schober KE, Bonagura JD. Echocardiographic evidence of left atrial mechanical dysfunction after conversion of atrial fibrillation to sinus rhythm in 5 horses. J Vet Intern Med 2007;21:820–827.

21. Sepulveda MF, Perkins JD, Bowen IM, et al. Demonstration of regional differences in equine ventricular myocardial velocity in normal 2-year-old Thoroughbreds with Doppler tissue imaging. Equine Vet J 2005;37:222–226.

22. Schwarzwald CC, Schober KE, Bonagura JD. Methods and reliability of echocardiographic assessment of left atrial size and mechanical function in horses. Am J Vet Res 2007;68:735–747.

23. Schwarzwald CC, Schober KE, Bonagura JD. Methods and reliability of tissue Doppler imaging for assessment of left ventricular radial wall motion in horses. J Vet Intern Med 2009;23:643–652.

24. Teske AJ, De Boeck BW, Melman PG, et al. Echocardiographic quantification of myocardial function using tissue deformation imaging—a guide to image acquisition and analysis using tissue Doppler and speckle tracking. Cardiovasc Ultrasound 2007;5:27–45.

25. Marwick TH. Measurement of strain and strain rate by echocardiography: Ready for prime time? J Am Coll Cardiol 2006;47:1313–1327.

26. Chetboul V. Tissue Doppler imaging: A promising technique for quantifying regional myocardial function. J Vet Cardiol 2002; 4:7–12.

27. Nikitin NP, Witte KK. Application of tissue Doppler imaging in cardiology. Cardiology 2004;101:170–184.

28. Chetboul V, Athanassiadis N, Carlos C, et al. Quantification, repeatability, and reproducibility of feline radial and longitudinal left ventricular velocities by tissue Doppler imaging. Am J Vet Res 2004;65:566–572.

29. Chetboul V, Athanassiadis N, Carlos C, et al. Assessment of repeatability, reproducibility, and effect of anesthesia on determination of radial and longitudinal left ventricular velocities via tissue Doppler imaging in dogs. Am J Vet Res 2004;65:909–915.

30. Perk G, Tunick PA, Kronzon I. Non-Doppler two-dimensional strain imaging by echocardiography—from technical considerations to clinical applications. J Am Soc Echocardiogr 2007;20: 234–243.

31. Artis NJ, Oxborough DL, Williams G, et al. Two-dimensional strain imaging: A new echocardiographic advance with research and clinical applications. Int J Cardiol 2008;123:240–248.

32. Schwarzwald CC, Schober KE, Berli AS, et al. Left ventricular radial and circumferential wall motion analysis in horses using strain, strain rate, and displacement by 2D speckle tracking. J Vet Intern Med 2009;23:890–900.

33. Becker M, Bilke E, Kuhl H, et al. Analysis of myocardial deformation based on pixel tracking in two dimensional echocardiographic images enables quantitative assessment of regional left ventricular function. Heart 2006;92:1102–1108.

34. Cheitlin MD, Alpert JS, Armstrong WF, et al. ACC/AHA guidelines for the clinical application of echocardiography: A report of the American College of Cardiology/American Heart Association task force on practice guidelines (committee on clinical application of Echocardiography). Developed in collaboration with the American Society of Echocardiography. Circulation 1997;95: 1686–1744.

35. Bellenger NG, Burgess MI, Ray SG, et al. Comparison of left ventricular ejection fraction and volumes in heart failure by echocardiography, radionuclide ventriculography and cardiovascular magnetic resonance; Are they interchangeable? Eur Heart J 2000;21:1387–1396.

36. Pluim BM, Beyerbacht HP, Chin JC, et al. Comparison of echocardiography with magnetic resonance imaging in the assessment of the athlete's heart. Eur Heart J 1997;18:1505–1513.

37. Wandt B. Long-axis contraction of the ventricles: A modern approach, but described already by Leonardo da Vinci. J Am Soc Echocardiogr 2000;13:699–706.

38. Rugh KS, Garner HE, Miramonti JR, et al. Left ventricular function and haemodynamics in ponies during exercise and recovery. Equine Vet J 1989;21:39–44.

39. Guyton AC, Hall JE. Heart muscle: The heart as a pump and function of the heart valves. In: Guyton AC, Hall JE, eds. Textbook of Medical Physiology, 11th ed. Philadelphia, PA: WB Saunders; 2006:103–122.

40. Yamada E, Garcia M, Thomas JD, et al. Myocardial Doppler velocity imaging—a quantitative technique for interpretation of dobutamine echocardiography. Am J Cardiol 1998;82:806–809.

41. Pasquet A, Armstrong G, Beachler L, et al. Use of segmental tissue Doppler velocity to quantitate exercise echocardiography. J Am Soc Echocardiogr 1999;12:901–912.

42. Quintana M, Saha SK, Rohani M, et al. Assessment of the longitudinal and circumferential left ventricular function at rest and during exercise in healthy elderly individuals by tissue-Doppler echocardiography: Relationship with heart rate. Clin Sci (Lond) 2004;106:451–457.

43. Bjallmark A, Larsson M, Shahgaldi K, et al. Differences in myocardial velocities during supine and upright exercise stress echocardiography in healthy adults. Clin Physiol Funct Imaging 2009; 29:216–223.

44. Atkins CE, Snyder PS. Systolic time intervals and their derivatives for evaluation of cardiac function. J Vet Intern Med 1992;6:55–63.

45. Stoylen A, Wisloff U, Slordahl S. Left ventricular mechanics during exercise: A Doppler and tissue Doppler study. Eur J Echocardiogr 2003;4:286–291.

46. Stoylen A.. Strain rate imaging: Cardiac deformation imaging by ultrasound/echocardiography—Tissue Doppler and speckle tracking. Trondheim, Norway: Website Content, 2008. Available at http://folk.ntnu.no/stoylen/strainrate/ (accessed October 20, 2009).

47. Weidemann F, Jamal F, Sutherland GR, et al. Myocardial function defined by strain rate and strain during alterations in inotropic states and heart rate. Am J Physiol Heart Circ Physiol 2002;283:H792–H799.

48. Marwick TH. Straining to detect ischaemia. Eur Heart J 2007;28:1407–1408.

49. Hamilton WF. Movements of the base of the ventricle and relative constancy of the cardiac volume. Am J Physiol 1932;102: 559–565.

50. Bogaert J, Rademakers FE. Regional nonuniformity of normal adult human left ventricle. Am J Physiol Heart Circ Physiol 2001;280:H610–H620.

51. Hamdan A, Thouet T, Kelle S, et al. Strain-encoded MRI to evaluate normal left ventricular function and timing of contraction at 3.0 Tesla. J Magn Reson Imaging 2009;29:799–808.

52. Voigt JU, Arnold MF, Karlsson M, et al. Assessment of regional longitudinal myocardial strain rate derived from Doppler myocardial imaging indexes in normal and infarcted myocardium. J Am Soc Echocardiogr 2000;13:588–598.

53. Sengupta PP, Khandheria BK, Korinek J, et al. Apex-to-base dispersion in regional timing of left ventricular shortening and lengthening. J Am Coll Cardiol 2006;47:163–172.

54. Berli ASJ, Jud R, Steininger K, Schwarzwald CC. The use of strain, strain rate, and displacement by 2D speckle tracking for assessment of systolic left ventricular function in goats: Applicability and influence of general anesthesia. In: Proceedings of the 27th Annual ACVIM Forum, Montreal, Quebec, Canada 2009.

55. Hamlin RL, Smith CR. Categorization of common domestic mammals based upon their ventricular activation process. Ann NY Acad Sci 1965;127:195–203.

56. Schwarzwald CC, Bonagura JD, Muir WW. The cardiovascular system. In: Muir WW, Hubell JAE, eds. Equine Anesthesia, 2nd ed. Philadelphia, PA: WB Saunders; 2009:37–100.

57. Picano E, Lattanzi F, Orlandini A, et al. Stress echocardiography and the human factor: The importance of being expert. J Am Coll Cardiol 1991;17:666–669.

58. Hoffmann R, Lethen H, Marwick T, et al. Analysis of interinstitutional observer agreement in interpretation of dobutamine stress echocardiograms. J Am Coll Cardiol 1996;27:330–336.

59. Hoffmann R, Marwick TH, Poldermans D, et al. Refinements in stress echocardiographic techniques improve interinstitutional agreement in interpretation of dobutamine stress echocardiograms. Eur Heart J 2002;23:821–829.

60. Edvardsen T, Aakhus S, Endresen K, et al. Acute regional myocardial ischemia identified by 2-dimensional multiregion tissue Doppler imaging technique. J Am Soc Echocardiogr 2000;13: 986–994.

61. Perk G, Kronzon I. Non-Doppler two dimensional strain imaging for evaluation of coronary artery disease. Echocardiography 2009;26:299–306.

62. Kukulski T, Jamal F, D'Hooge J, et al. Acute changes in systolic and diastolic events during clinical coronary angioplasty: A comparison of regional velocity, strain rate, and strain measurement. J Am Soc Echocardiogr 2002;15:1–12.

63. Abraham TP, Belohlavek M, Thomson HL, et al. Time to onset of regional relaxation: Feasibility, variability and utility of a novel index of regional myocardial function by strain rate imaging. J Am Coll Cardiol 2002;39:1531–1537.

64. Gorcsan J, Abraham T, Agler DA, et al. Echocardiography for cardiac resynchronization therapy: Recommendations for performance and reporting—a report from the American Society of Echocardiography Dyssynchrony writing group endorsed by the Heart Rhythm Society. J Am Soc Echocardiogr 2008;21:191–213.

65. Arita T, Sorescu GP, Schuler BT, et al. Speckle-tracking strain echocardiography for detecting cardiac dyssynchrony in a canine model of dyssynchrony and heart failure. Am J Physiol Heart Circ Physiol 2007;293:H735–H742.

66. Delgado V, Ypenburg C, van Bommel RJ, et al. Assessment of left ventricular dyssynchrony by speckle tracking strain imaging—comparison between longitudinal, circumferential, and radial strain in cardiac resynchronization therapy. J Am Coll Cardiol 2008;51:1944–1952.